Electron density and temperature-sensitive x-ray-emission-line ratios for heliumlike Si XIII in the DITE tokamak

F. P. Keenan and S. M. McCann

Department of Pure and Applied Physics, Queen's University, Belfast BT7 1NN, Northern Ireland

R. Barnsley, J. Dunn, and K. D. Evans

Department of Physics, University of Leicester, Leicester LE1 7RH, England

N. J. Peacock

Culham Laboratory, Oxford OX14 3DB, England

(Received 31 August 1988)

Recent calculations of electron impact excitation rates in heliumlike Si XIII are used to derive the electron-density-sensitive emission-line ratio R $(=f/i)$ and temperature-sensitive ratio G $[=(f+i)/r]$, where f, i, and r are the forbidden $1s^2\,^1S-1s2s\,^3S$, intercombination $1s^2\,^1S-1s2p\,^3P_{1,2}$ and resonance $1s^2\,^1S-1s2p\,^1P$ transitions, respectively. A comparison of these with R and G ratios measured from x-ray spectra of the divertor injected tokamak experiment, for which the electron density and temperature have been well determined, reveals good agreement between theory and observation, with discrepancies of typically 8% in R and 5% in G. This provides experimental support for the accuracy of the atomic data adopted in the line ratio calculations. The theoretical results may be applied to the analysis of remote sources for which no independent electron density and temperature estimates exist (such as solar flares), in order to derive values of N_e and T_e which, on the basis of the above comparison between theory and observation, should be accurate to ±0.3 and ±0.1 in the log, respectively.

I. INTRODUCTION

Emission lines arising from transitions between the $1s^2\,^1S$ ground state and the $1s2l$ levels in heliumlike ions are frequently observed in the x-ray spectra of high-temperature laboratory plasmas,[1,2] as well as the solar corona.[3-5] They may be used to infer the electron density and temperature of the emitting region through the well-known line ratios R $(=f/i)$ and G $[=(f+i)/r]$ respectively, where f is the forbidden $1s^2\,^1S-1s2s\,^3S$ transition, i the intercombination $1s^2\,^1S-1s2p\,^3P_{1,2}$ lines and r the resonance $1s^2\,^1S-1s2p\,^1P$ transition.[6-8] However, to determine reliable theoretical ratios, accurate atomic physics data must be employed, especially for electron excitation rates and f values.[9]

Over the past few years several authors have calculated electron-impact excitation rates for He-like ions. Probably the most accurate currently available are those for C V, O VII, and Mg XI derived with the R-matrix code[10] by Tayal and Kingston,[11-17] and the results for Ca XIX and Fe XXV estimated by Pradhan[18] in the distorted-wave approximation.[19,20] Keenan, Doyle, and co-workers[21-30] have shown that the theoretical R and G ratios determined using either the above atomic data or excitation rates for other He-sequence members interpolated from these[31] are in much better agreement with solar active region and flare observations than are previous calculations.[32-34]

For He-like ions with atomic numbers $Z > 12$, the R ratio is in its low-density limit for values of N_e ($\leq 10^{12}$ cm^{-3}) typically found under solar conditions.[34] Howev-

er, this is not the case with tokamak laboratory plasmas, where the densities may be several orders of magnitude larger,[35] and hence R in high-Z species should be useful as an electron-density diagnostic. In this paper we use the Keenan et al.[31] excitation-rate calculations for Si XIII to derive R and G ratios for this ion, and compare these with observational data from the divertor injected tokamak experiment (DITE). Hence we investigate if the current discrepancies between theory and observation for heliumlike ions in tokamak spectra may be resolved.[36]

II. ATOMIC DATA

The model ion for Si XIII was similar to those adopted for other He-like ions by Keenan and his co-workers.[22-29] Briefly, the 23 $1snl$ states with $n < 6$ and $l < 3$ were included in the calculations, making a total of 37 levels when the fine-structure splitting in the ^3P and ^3D terms was included. Energies of these levels were taken from Martin and Zalubas.[37]

Electron-impact excitation rates from the $1s^2\,^1S$ ground state to the $n = 2$ and 3 levels were obtained from Keenan et al.,[31] while for those among $n = 2$ the results of Pradhan et al.[38] and Zhang and Sampson[39] were adopted. Rates to or between higher $1snl$ states were either estimated from the above using the n^{-3} scaling law[40] or taken from Sampson et al.[41]

Einstein A coefficients for transitions from the $n = 2$ levels were obtained from Lin et al.,[42] the results of Lin et al.[43] and Cohen and McEachran[44] being used for $n > 2$. As noted by, for example, Blumenthal et al.[7] and

Pradhan,[33] inner-shell ionization of the Li-like ion and dielectronic and radiative recombination of the H-like ion are important mechanisms in determining the level populations of the relevant He-like ion. We have included these processes in the present analysis by employing the rate coefficients of Mewe and Schrijver[45] in conjunction with the Si XII–Si XIII–Si XIV ionization balance calculations of Arnaud and Rothenflug.[46]

As has been discussed by, for example, Seaton,[47] proton excitation may be important for transitions with small excitation energies, i.e., fine-structure transitions such as that in the $2s^2 2p^5\,^2P$ term in Fe XVIII.[48] However, test calculations with Si XIII setting the proton rates for $1s2p\,^3P_J - 1s2p\,^3P_{J'}$ transitions equal to the corresponding electron excitation rates or ten times these values had a negligible effect on the level populations, and hence this atomic process was not included in the present analysis.

III. EXPERIMENTAL DATA

The experimental results were obtained from the DITE and tokamak at the United Kingdom Atomic Energy Authority, Culham Laboratory.[49] This tokamak has major and minor radii of 1.2 and 0.24 m, respectively, a maximum toroidal field of 2.7 T, and maximum toroidal current of 300 kA. The central electron density can be varied between about $N_e \simeq 5 \times 10^{12}$ and $\leq 10^{14}$ cm^{-3}, and the central electron temperature between about 500 and 1000 eV. The highest densities in this range can only be achieved in helium plasmas. Small concentrations (typically 0.01% of N_e) of Si ions were added to the plasma by sputtering from samples placed in the scrape-off layer by an adjustable probe. The central-chord integrated electron density was measured with a microwave interferometer,[49] while radial profiles of electron density and temperature were determined by Thomson scattering of a 2-J ruby laser.[50]

Most of the spectra were obtained with a Bragg rotor spectrometer,[51] which had absolute calibration for flux and wavelength, and used a slotted (Soller) collimator to
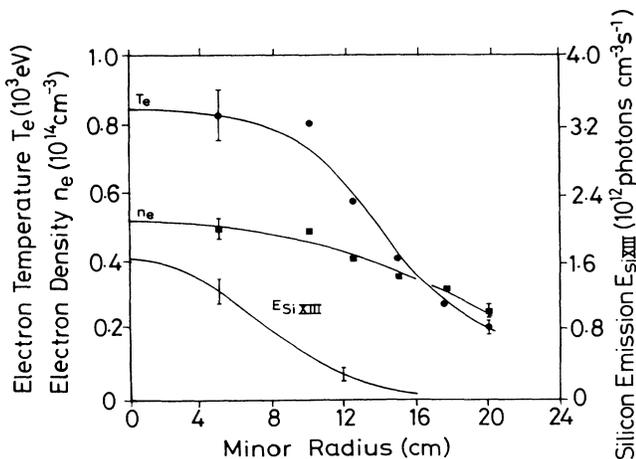
achieve a resolving power $(\lambda/\delta\lambda)$ of between 200 and 2000. A hexagonal rotor supported six interchangeable crystals and could be locked in a monochromator mode, or rotated at up to 10 Hz for spectral surveys. The detector was a multiwire gas proportional counter which could operate at count rates up to 10 MHz. All spectrometer functions and data acquisition were computer controlled, and radial profiles could be obtained by tilting the spectrometer vacuum system on a shot-to-shot basis. The resolving power depended on the combination of collima-
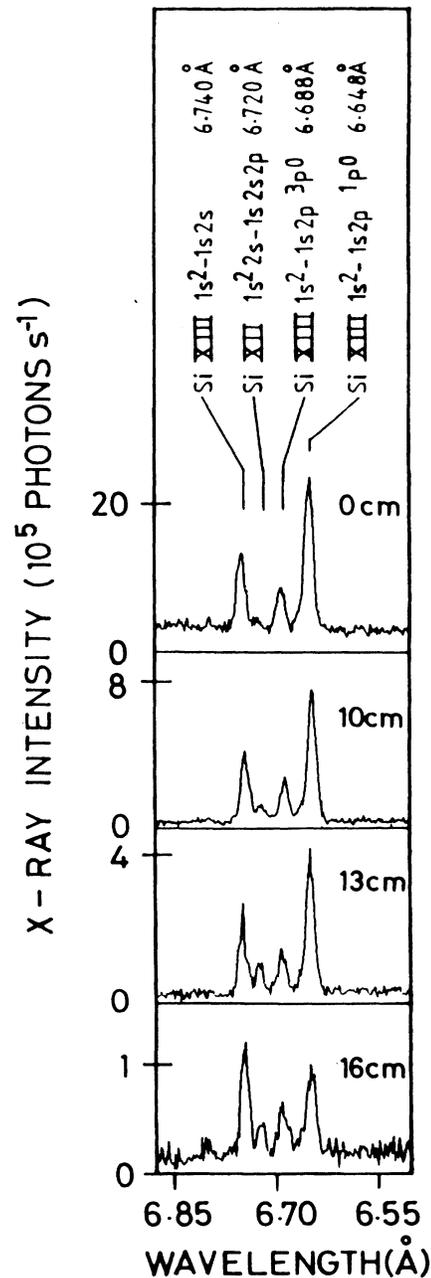

FIG. 2. Radial dependence of He-like silicon. At the outer radii the relative intensity of the $1s^2\,^1S - 1s2p\,^1P$ line decreases, and at the most extreme radii only the forbidden line remains.
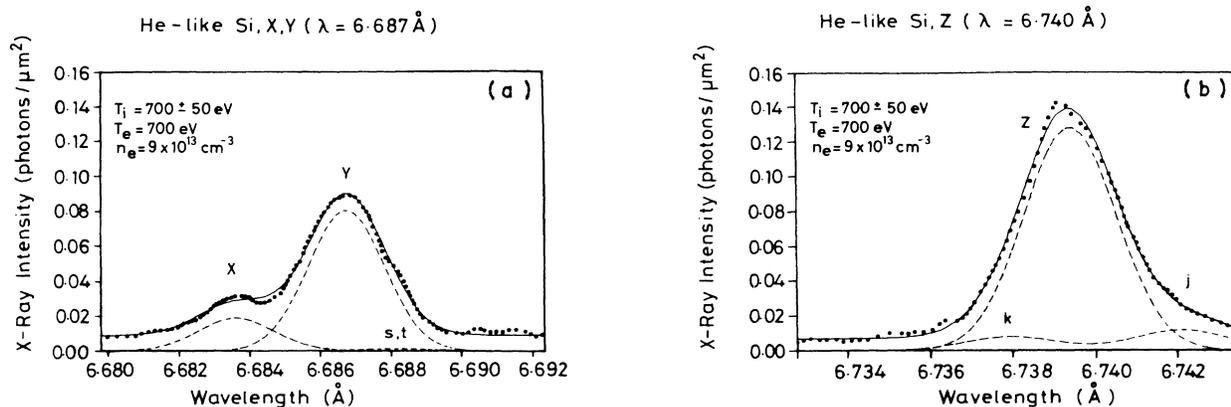

FIG. 1. Radial profiles of the electron temperature (T_e), the electron density (n_e), and the Si XIII emission profile ($E_{\text{Si XIII}}$).

FIG. 3. (a) and (b) High-resolution spectra of the He-like silicon $1s^2\,{}^1S-1s2p\,{}^3P_{1,2}$ intercombination (X, Y) and the $1s^2\,{}^1S-1s2s\,{}^3S$ forbidden (Z) lines, respectively. A least-squares fit (solid lines) to the experimental points (solid points), using a Voigt profile routine which includes the crystal diffraction width, (Ref. 54), gives good agreement if the unresolved dielectronic satellite lines (Ref. 55) are included. Individual contributions to the line intensity are indicated (dashed lines). For these plasma conditions of $n_e = 9 \times 10^{13}$ cm^{-3} and $T_e = 700$ eV, the observed forbidden line intensity is enhanced by 13% due to the satellite lines j and k [labeled according to Gabriel (Ref. 60)]. The satellite lines s and t under the intercombination lines are less significant. An ion temperature $T_i = 700$ eV is calculated from the Doppler width of the forbidden and intercombination lines.

tor, crystal and Bragg angle, and for the Si XIII observations was about 600.

Further Si XIII spectra, resolved to about 1 part in 2400 (limited by thermal Doppler broadening), were recorded on Kodak DEF film with a curved crystal Johann spectrometer.[52] These better-resolved spectra allowed an estimate of the contribution of satellite lines to the Si XIII spectrum, and were used to correct the R and G ratio measurements.

The tokamak has an approximately parabolic electron-density radial profile (Fig. 1), and in principle

use could be made of the density gradient to study the R ratio as a function of N_e, by making a radial scan of the spectrum. This technique is complicated by the steep T_e profile (Fig. 1), which means that the density scan would not be at constant T_e. A more serious drawback is caused by transport of fully stripped and H-like ions from the plasma core to the cooler outer regions beyond a $\sim$12-cm minor radius. This transport takes place on a time scale similar to the recombination time, and results in a nonthermal ionization balance, and a spectrum in the outer region of the plasma which is dominated by recom-
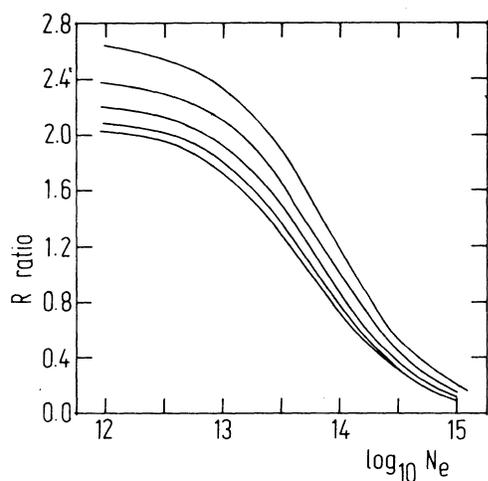

FIG. 4. The theoretical emission line ratio R (line intensities in photons) plotted as a function of electron density at electron temperature of (from bottom to top), $\log_{10}T_e = 6.4$, 6.6, 6.8, 7.0, and 7.2 (T_e in units of degrees Kelvin), with dielectronic and radiative recombination and inner-shell ionization included in the calculations.
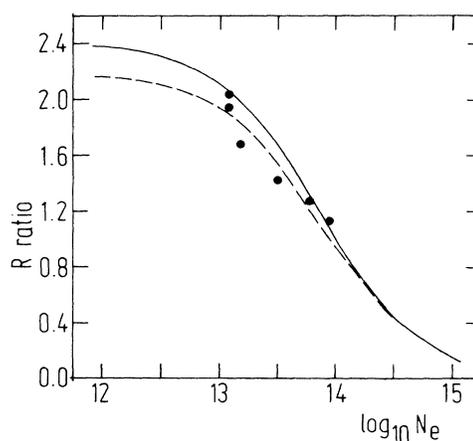

FIG. 5. The theoretical emission line ratio R (line intensities in photons) plotted as a function of electron density at the temperature of maximum Si XIII emissivity, $\log_{10}T_m = 7.0$ (Ref. 58), with dielectronic and radiative recombination and inner-shell ionization either included in (solid line) or excluded from (dashed line) the calculations. Typical errors in the experimental data (solid points) are $\pm 9\%$ in R'_{obs} and ± 0.02 in $\log_{10}N_e$.

bination rather than electron impact excitation. This effect has been observed for Ar XVII in the Alcator tokamak,[53] and for lighter ions such as Si XIII in DITE. At the outer radii the relative intensity of the $1s^2\,{}^1S - 1s2p\,{}^1P$ line decreases (Fig. 2), and at the most extreme radii only the forbidden line remains.

The present results were recorded over almost the full density range of DITE so that at each density the ions could be observed in the center of plasma, where there is approximate coronal equilibrium. (Radial profiles of the Si XIV-to-Si XIII emission ratio gave good agreement with coronal equilibrium for radii less than about 10 cm). Examination of the spatial Si XIII emission profile (Fig. 1) shows that almost all of the emission is from the central region of the plasma, where N_e is almost constant and T_e does not vary significantly. The range of N_e and T_e from which the central-chord signal is emitted is similar to the error in the measurement of the central values, i.e., about 10% for T_e and 5% for N_e. This localization of the emission allows the R and G ratios to be measured from the central-chord integrated signal alone, without the need for radial profiles at every plasma density.

In deriving the R and G ratios, account was taken of the charge in spectrometer sensitivity through the spectrum. An increase in sensitivity of about 7% is calculated between the resonance and forbidden lines, mainly due to the change in the Bragg reflection integral of the Pentaerythritol(002) crystal.[54]

The contribution of unresolved satellites was estimated from the high resolution spectrum [Figs. 3(a) and 3(b)], which shows that there are significant satellites blended in the less-well-resolved spectra from which the R and G ratios were measured (Fig. 2). The strongest dielectronic satellites at 6.74 Å are effectively unresolvable from the forbidden line, and their contribution has been calculated to be 13% of the observed forbidden line.[55] The satellite contribution to the intercombination lines is only a few percent and is less significant.

IV. RESULTS AND DISCUSSION

Using the statistical equilibrium code of Dufton[56] with the atomic data discussed in Sec. II, relative level populations and hence emission line strengths for Si XIII were estimated, where the following assumptions were made: (i) that photoexcitation and deexcitation rates are negligible in comparison with the corresponding collisional rates, and (ii) that all transitions are optically thin. Further de-

tails of the procedures involved may be found in Dufton[56] and Dufton et al.[57]

In Fig. 4 the theoretical R ratio is shown for values of electron density $(N_e \simeq 10^{12}-10^{15}$ cm$^{-3})$ typical of tokamak plasmas, at several temperatures between $\log_{10}T_e = 6.4$ and 7.2 $(T_e$ in units of degrees Kelvin), where Si XIII has a significant abundance in ionization equilibrium.[46] The potential usefulness of the ratio as a density diagnostic is clear from the figure, as it varies by approximately a factor of 16 between $\log_{10}N_e = 12.0$ and 15.0. Furthermore, it is relatively insensitive to electron temperature with, for example, a factor of 4 change in T_e resulting in a 30% or less variation in R.

The sensitivity of R to recombination processes is illustrated in Fig. 5, where the ratio is plotted as a function of N_e at the temperature of maximum Si XIII emissivity, $\log_{10}T_m = 7.0$.[58] It can be seen that the effect of recombination on R is quite small, increasing its value by only about 10% in the low-density limit.

The theoretical G ratio is plotted in Fig. 6 as a function of electron temperature at a density $N_e = 10^{13}$ cm^{-3}. We note that although G becomes density sensitive at high values of N_e, decreasing due to quenching of the two photon $1s^2\,{}^1S - 1s2s\,{}^1S$ transition by collisional excitation of $1s2s\,{}^1S$ to the $1s2p\,{}^1P$ state,[30] this is not the case for the densities considered in the present analysis. For example, at $\log_{10}T_e = 7.0$ the values of G are 0.72 and 0.71 for $\log_{10}N_e = 12.0$ and 15.0, respectively. An inspection of Fig. 6 shows that the effects of recombination on G are much larger than on R, increasing the former by approximately 25% at $\log_{10}T_e = 6.8$ and 60% at $\log_{10}T_e = 7.2$.

In Table I we compare the theoretical and observed values of R and G, and the comparison is also shown graphically in Figs. 5 and 6. [We note that the observed electron temperatures all lie within 0.1 dex of $\log_{10}T_e = 7.0$, and as R is not strongly dependent on T_e (see above), it is hence justifiable to plot the experimental R ratios on one R versus $\log_{10}N_e$ curve]. The high-resolution data, obtained over limited N_e conditions but constant T_e, were used to correct the low-resolution observations for the presence of satellites over the larger range of N_e conditions. In Table I the uncorrected and corrected R ratios are labeled R_{obs} and R'_{obs}, respectively, and the latter have been used in Fig. 5. However, we note that applying the same technique to the G ratio left it effectively unchanged, as the $n \geq 3$ satellites close to and under the resonance line contribute proportionally the same as the satellites under the forbidden and inter-

TABLE I. Comparison of observed and theoretical Si XIII R and G ratios. R_{obs} and R'_{obs} are the observed values of R uncorrected and corrected for the presence of satellite lines, respectively.

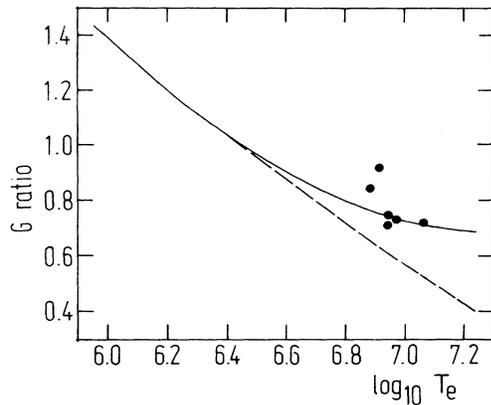| N_e (10^{13} cm^{-3})	T_e (eV)	Number of spectra	R_{obs}	R'_{obs}	R_{theory}	G_{obs}	G_{theory}
3.0	750	2	1.59	1.42	1.63	0.71	0.74
1.2	800	3	2.13	1.94	2.03	0.73	0.73
9.0	700	3	1.28	1.13	1.01	0.92	0.76
1.5	750	4	1.86	1.68	1.92	0.74	0.74
1.2	1000	2	2.23	2.03	2.12	0.72	0.71
6.0	650	2	1.43	1.27	1.26	0.84	0.77

FIG. 6. The theoretical emission line ratio G (line intensities in photons) plotted as a function of electron temperature T_e (in units of degrees Kelvin) at an electron density of $\log_{10} N_e = 13.0$, with dielectronic and radiative recombination and inner-shell ionization either included in (solid line) or excluded from (dashed line) in the calculations. Typical errors in the experimental data (solid points) are $\pm 6\%$ in G_{obs} and ± 0.04 in $\log_{10} T_e$.

combination lines at these electron temperatures. Hence only the uncorrected G ratios G_{obs} are listed in Table I.

An inspection of Table I and Figs. 5 and 6 reveals that the agreement between the experimental and theoretical results is good, with discrepancies of typically 8% and 5% in R and G, respectively, which provides support for the accuracy of the atomic data adopted in the line ratio calculations. These differences correspond to changes of approximately 0.3 dex in the electron density and 0.1 dex in the temperature. Hence, using the theoretical results in Figs. 4 and 6, plasma parameters to these levels of accuracy may in principle be derived for remote sources for which no independent estimates of N_e and T_e exist, such as the solar flare x-ray spectra obtained with the P78-1 (Ref. 26) and Solar Maximum Mission[59] satellites.

Finally, we note that the experimental R ratios in Si XIII only vary by about a factor of 2 over the investigated density range from $1.2 \times 10^{13} - 9.0 \times 10^{13}$ cm^{-3} (Fig. 5). However, for heliumlike Mg XI the predicted variations in R over a similar density interval are much larger [approximately a factor of 5 (Ref. 22)]. It would therefore be of great interest to study the spectra of Mg XI in DITE plasmas, in order to demonstrate that the forbidden line for this ion is indeed suppressed at high density as predicted by theory.

ACKNOWLEDGMENTS

[1]P. Lee, A. J. Lieber, A. K. Pradhan, and Y. Xu, Phys. Rev. A **34**, 3210 (1986).

[2]K. H. Kolk, R. Konig, and H. J. Kunze, Phys. Rev. A **33**, 747 (1986).

[3]D. L. McKenzie, P. B. Landecker, U. Feldman, and G. A. Doschek, Astrophys. J. **289**, 849 (1985).

[4]K. J. H. Phillips et al., Astrophys. J. **256**, 774 (1982).

[5]L. W. Acton, M. E. Bruner, W. A. Brown, B. C. Fawcett, W. Schweizer, and R. J. Speer, Astrophys. J. **291**, 865 (1985).

[6]A. H. Gabriel and C. Jordan, Mon. Not. R. Astron. Soc. **145**, 241 (1969).

[7]G. T. Blumenthal, G. W. F. Drake, and W. H. Tucker, Astrophys. J. **172**, 205 (1972).

[8]L. W. Acton and W. A. Brown, Astrophys. J. **225**, 1065 (1978).

[9]A. H. Gabriel and C. Jordan, Case Stud. At. Phys. **2**, 209 (1972).

[10]P. G. Burke and W. D. Robb, Adv. At. Mol. Phys. **11**, 143 (1975).

[11]A. E. Kingston and S. S. Tayal, J. Phys. B **16**, L53 (1983).

[12]A. E. Kingston and S. S. Tayal, J. Phys. B **16**, 3465 (1983).

[13]S. S. Tayal and A. E. Kingston, J. Phys. B **17**, L145 (1984).

[14]S. S. Tayal and A. E. Kingston, J. Phys. B **17**, 1383 (1984).

[15]S. S. Tayal and A. E. Kingston, J. Phys. B **18**, 2983 (1985).

[16]S. S. Tayal, Phys. Rev. A **34**, 1847 (1986).

[17]S. S. Tayal, Phys. Rev. A **35**, 2073 (1987).

[18]A. K. Pradhan, Astrophys. J. Suppl. Ser. **59**, 183 (1986).

[19]W. Eissner and M. J. Seaton, J. Phys. B **5**, 2178 (1972).

[20]H. E. Saraph, Comput. Phys. Commun. **3**, 256 (1972).

[21]J. G. Doyle, S. S. Tayal, and A. E. Kingston, Mon. Not. R. Astron. Soc. **203**, 31P (1983).

[22]F. P. Keenan, S. S. Tayal, and A. E. Kingston, Mon. Not. R. Astron. Soc. **207**, 51P (1984).

[23]F. P. Keenan, S. S. Tayal, and A. E. Kingston, Solar Phys. **92**, 75 (1984).

[24]F. P. Keenan, S. S. Tayal, and A. E. Kingston, Solar Phys. **94**, 85 (1984).

[25]J. G. Doyle and F. P. Keenan, Astron. Astrophys. **157**, 116 (1986).

[26]S. M. McCann and F. P. Keenan, Solar Phys. **112**, 83 (1987).

[27]F. P. Keenan and S. M. McCann, Solar Phys. **109**, 31 (1987).

[28]S. M. McCann and F. P. Keenan, Astrophys. J. **328**, 344 (1988).

[29]F. P. Keenan, D. L. McKenzie, S. M. McCann, and A. E. Kingston, Astrophys. J. **318**, 926 (1987).

[30]D. L. McKenzie, Astrophys. J. **322**, 512 (1987).

[31]F. P. Keenan, S. M. McCann, and A. E. Kingston, Phys. Scr. **35**, 432 (1987).

[32]A. K. Pradhan and J. M. Shull, Astrophys. J. **249**, 821 (1981).

[33]A. K. Pradhan, Astrophys. J. **263**, 477 (1982).

[34]C. J. Wolfson, J. G. Doyle, J. W. Leibacher, and K. J. H. Phillips, Astrophys. J. **269**, 319 (1983).

[35]J. E. Rice, E. S. Marmar, E. Källne, and J. Källne, Rev. Sci.

Instrum. **57**, 2154 (1986).

[36]T. Kato, S. Morita, K. Masai, and S. Hayakawa, Phys. Rev. A **36**, 795 (1987).

[37]W. C. Martin and R. Zalubas, J. Phys. Chem. Ref. Data **12**, 323 (1983).

[38]A. K. Pradhan, D. W. Norcross, and D. G. Hummer, Astrophys. J. **246**, 1031 (1981).

[39]H. Zhang and D. H. Sampson, Astrophys. J. Suppl. Ser. **63**, 487 (1987).

[40]A. H. Gabriel and D. W. O. Heddle, Proc. R. Soc. London, Ser. A **258**, 124 (1960).

[41]D. H. Sampson, S. J. Goett, and R. E. H. Clark, At. Data Nucl. Data Tables **29**, 467 (1983).

[42]C. D. Lin, W. R. Johnston, and A. Dalgarno, Phys. Rev. A **15**, 154 (1977).

[43]C. D. Lin, W. R. Johnston, and A. Dalgarno, Astrophys. J. **217**, 1011 (1977).

[44]M. Cohen and R. P. McEachran, Can. J. Phys. **50**, 1363 (1972).

[45]R. Mewe and J. Schrijver, Astron. Astrophys. **65**, 99 (1978).

[46]M. Arnaud and R. Rothenflug, Astron. Astrophys. Suppl. Ser. **60**, 425 (1985).

[47]M. J. Seaton, Mon. Not. R. Astron. Soc. **127**, 191 (1964).

[48]F. P. Keenan and R. H. G. Reid, J. Phys. B **20**, L753 (1987).

[49]J. M. Allen *et al.*, Plasma Phys. Controlled Fusion **28**, 101 (1986).

[50]R. Prentice, Culham Laboratory Report No. CLM R179, 1978 (unpublished).

[51]R. Barnsley, K. D. Evans, N. C. Hawkes, and N. J. Peacock, J. Phys. (Paris) **49**, 207 (1988).

[52]J. Dunn, R. Barnsley, K. D. Evans, and N. J. Peacock, J. Phys. (Paris) **49**, 91 (1988).

[53]J. E. Rice, E. S. Marmar, E. Källne, and J. Källne, Phys. Rev. A **35**, 3033 (1987).

[54]R. Hall, Ph.D. thesis, University of Leicester, 1980 (unpublished).

[55]J. Nilsen, At. Data Nucl. Data Tables **38**, 339 (1988).

[56]P. L. Dufton, Comput. Phys. Commun. **13**, 25 (1977).

[57]P. L. Dufton, K. A. Berrington, P. G. Burke, and A. E. Kingston, Astron. Astrophys. **62**, 111 (1978).

[58]R. Mewe, E. H. B. M. Gronenschild, and G. H. van den Oord, Astron. Astrophys. Suppl. Ser. **62**, 197 (1985).

[59]F. P. Keenan, S. M. McCann, K. J. H. Phillips, and B. J. I. Bromage (unpublished).

[60]A. H. Gabriel, Mon. Not. R. Astron. Soc. **160**, 99 (1972).